

immense and lasting value for astronomical research, now and in the future. Sky surveys and patrols must continue, lest future generations of astronomers will blame us for not having done our historical duty. When carefully processed and properly stored, photographic plates can last for centuries, while there is at the present no guarantee that even a fraction of the many CCD frames obtained during the past ten years will also be accessible, say, 100 years from now.

It must be stressed that the present conclusion does not apply to work at lower angular resolution and with small

er instruments; there are several examples of the great utility of wide-angle CCD work, for instance the extensive monitoring of Comet Halley's CO⁺ tail with a 640 × 1024 pix² camera at La Silla in 1986. *It would be highly desirable in the future to complement large Schmidt surveys with very-wide field patrol exposures by specialized low-resolution CCD cameras.*

There is little doubt that CCDs and other digital detectors will ultimately replace the photographic plates in all instruments, and also in the large Schmidt telescopes. But this step should only be taken when these detectors have be-

come big enough not to compromise the efficient and exhaustive exploitation of the unique scientific capabilities of wide-field Schmidt work and when the CCD archiving problem has been satisfactorily resolved.

Acknowledgements

I am very thankful to Martin Cullum, Bo Reipurth, Massimo Tarenghi and Edwin Valentijn, who suggested a number of important improvements to this article.

CASPEC's New Look

L. PASQUINI and A. GILLIOTTE, ESO, La Silla

1. Introduction

CASPEC, the 3.6-m Cassegrain Echelle Spectrograph, is one of the 4 high-resolution (HR) spectrographs presently available at La Silla. Together with the EMMI high-resolution mode, CASPEC is the only HR spectrograph capable of reaching relatively faint objects and, thanks to the crossdispersed orders, to record large wavelength ranges (up to 1400 Å in the present configuration) in only one frame. Since the high-resolution mode of EMMI is available in the RED arm only (i.e. for wavelengths redder than 4000 Å) CASPEC will probably remain for the next years the only HR spectrograph available at La Silla capable of reaching faint objects in the BLUE and in the near UV. Recently it has been successfully used at wavelengths as blue as 3130 Å (Baade and Crane, 1991).

ESO has started a programme to upgrade the instrument in order to increase the performance of CASPEC; we report here the recent improvements and we anticipate some of the changes foreseen before the end of the year. For a general description of the instrument the reader is referred to the ESO CASPEC Operating Manual (Pasquini and D'Odorico, 1989).

2. The New Detector

Since September 1990 a new detector is available for CASPEC: it is a 512 × 512 Tektronix chip (ESO CCD 16), with a pixel size of 27 × 27 μm. Its characteristics and response curve are given in Figure 1 (Sinclair, 1991).

This chip is in several aspects much better than the old RCA 8, previously mounted on CASPEC; in particular:

- It has a larger format, which allows a wavelength coverage up to ~ 1400 Å in one frame.

- It has a lower Read-Out Noise (RON) (~ 10 e⁻ compared to ~ 28 e⁻). This greatly increases the instrumental performance for low S/N observations, where the RON is the dominant source of noise.

- It has a very good cosmetic, no offset columns and no interference fringes; all these characteristics are essential for the correct reduction of Echelle data.

The efficiency of CASPEC with the 31.6 lines/mm echelle plus short camera and CCD 16 was measured through wide slit (4 × 4 arcsec) observations of the standard star Feige 56 (Stone, 1977); results are presented in Figure 2. We note that, in order to compute the data points of Figure 2, the echelle orders were not merged: electrons at wavelengths appearing in more than one order were measured separately and then added up.

The CCD response curve shown in Figure 1 was obtained after UV flooding, a procedure which enhances the detector sensitivity at wavelengths below ~ 4300 Å. When the efficiency tests were performed, the UV-flooding was not properly working; as a consequence, the points of Figure 2 in the Blue and UV ranges must be considered only as lower limits to the real instrumental efficiency.

The points of Figure 2 must be taken as indicative only, because when considering a real science exposure, possible slit losses must be taken into account. With this configuration, however, these losses are not expected to be very important; in fact, a good spectral sampling (2 pixels FWHM) is obtained with a slit width of ~ 300 μm,

which corresponds to 2.12 arcsec on the sky. This aperture is much wider than the typical seeing registered at the 3.6-m telescope.

In Figure 3, the expected S/N per pixel as a function of the integration time and the stellar magnitude is shown (continuous lines). In our calculations the stellar light was considered to spread over 3 pixels in the direction perpendicular to the dispersion (one Tektronix pixel corresponding to 0.648 arcsec in the sky with the short camera) and an airmass equal to 1. We fixed the CCD RON to 10 e⁻/pixel (instead of the nominal 8.8) because this value seems to be the most common at the telescope.

In Figure 3 are also plotted similar curves computed for the RCA (dashed lines, Pasquini and D'Odorico 1989); despite the lower quantum efficiency of the Tektronix with respect to the RCA, its bigger pixel size and lower RON allows to reach fainter objects.

The new chip, on the other hand, suffers some limitations, the knowledge of which is important for the users:

- The 27 μ pixel size limits the maximum achievable resolving power to R ~ 18,000 with the Short Camera.

- With the Long Camera a resolving power almost two times higher can be obtained, but with no order overlap. In such a configuration, in fact, the portion of the spectrum covered by each order is only 46 % of the wavelength ranges reported in the Thorium-Argon reference spectrum (D'Odorico et al., 1987). By tilting the crossdisperser it is possible to observe any portion of the orders (i.e. not necessarily the central part), but this adjustment can be made only in the afternoon, during the set-up procedure and it cannot be changed by the observer during the night.

- After saturation the CCD shows some remnants, which may last up to a few hours: special care (in particular in taking flat fields) should be used in order to avoid overexposure.

3. Filters

Partially related to the installation of the new chip is the choice of the filters now inserted in the filter wheels:

Neutral Density (ND) Filters: because the internal quartz lamp used for Flat Fields is rather red, it was impossible to obtain low- to intermediate-level flat fields for wavelengths above $\sim 5500 \text{ \AA}$ with the filters previously used. We have therefore inserted a higher density filter; Table 1 displays the new ND wheel configuration.

Colour Filters (CF): Three new colour filters were inserted, mostly to facilitate flat fielding in the BLUE and in the UV. The response curves of the available colour filters are shown in Figure 4. The new CF wheel has the following configuration:

Filter 1: (RG630, unchanged): It is a Long-Wavelength Passband (LWP), to be used for Th-Ar exposures at wavelengths longer than 6250 \AA in order to avoid possible contamination from second-order strong lines.

Filter 2: (DG530, unchanged) As filter 1, but with a cut-off at 5350 \AA .

Filter 3: (BG24) This filter is particularly important for Flat Fields at central wavelengths between ~ 4000 and $\sim 5000 \text{ \AA}$: it lowers the instrumental response in the red part of the spectrum, avoiding a too strong intensity gradient between the bluest and reddest orders.

Filters 4 and 5: (UG5 and BG3) As filter 3, but used for bluer wavelengths.

Colour filters can also be inserted in front of the rear-slit viewer and of the small-field cameras. Those filters are mostly recommended for observations in the UV and in the INFRARED in order to avoid miscentring due to the differential atmospheric refraction. The TV cameras have a spectral response peaked in the visible part of the spectrum. These filters can be used only on relatively bright sources. For these observations and for observations requiring very precise positioning of the object

TABLE 1: New ND wheel configuration.

Wheel position	Neutral density	Colour filter
1	2.22	RG 630
2	1.91	OG 530
3	1.37	BG 24
4	0.87	UG 5
5	0.51	BG 3

Chip Characteristics

Type:	Tektronix TEK 512M-12, thinned, backside illuminated.
Serial Number:	1215-3-8 (806-7468-71).
Format:	512×512 pixels, 50 pre-scan pixels in the horizontal direction.
Pixel size:	27×27 microns.
Image size:	13.8×13.8 mm.
Conversion factor:	Normally used at $1.7 \text{ e}^-/\text{ADU}$ (Gain 20, HCK=12 on Gen V Camera).
Noise level:	app. 8.8 e^- RMS at Gain 20 (HCK=12).
Linearity:	Better than $\pm 1 \%$. CCD saturation is about $100,000 \text{ e}^-/\text{pix}$.
Blemishes:	There are 3 parallel traps to be mapped.
Dark current:	The mean dark is app. $12 \text{ e}^-/\text{pix}/\text{hr}$ at 180 K.
Charge Transfer Eff.:	Measured CTE is 0.999993 in both directions (i.e. 99.3 % after 1000 transfers).
R.Q.E.:	Measured at 180 K. See below.
Operating temp.:	180 Kelvin.
Cosmic Ray Events:	$2.9 \pm 0.3 \text{ events}/\text{min}/\text{cm}^2$, i.e. app. 333 events/hr for the entire chip.

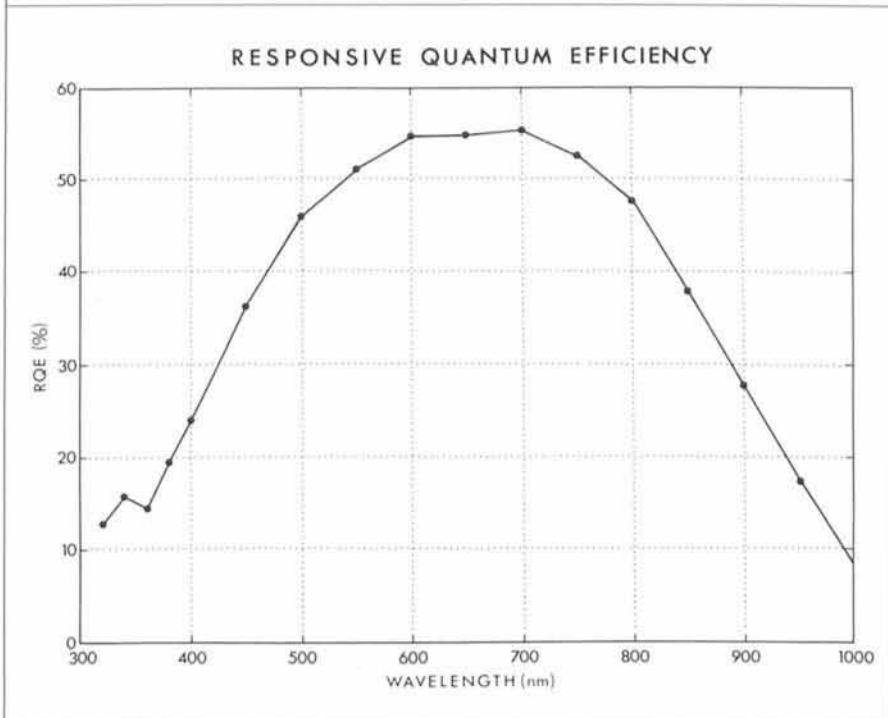


Figure 1: CCD 16 characteristics and response curve.

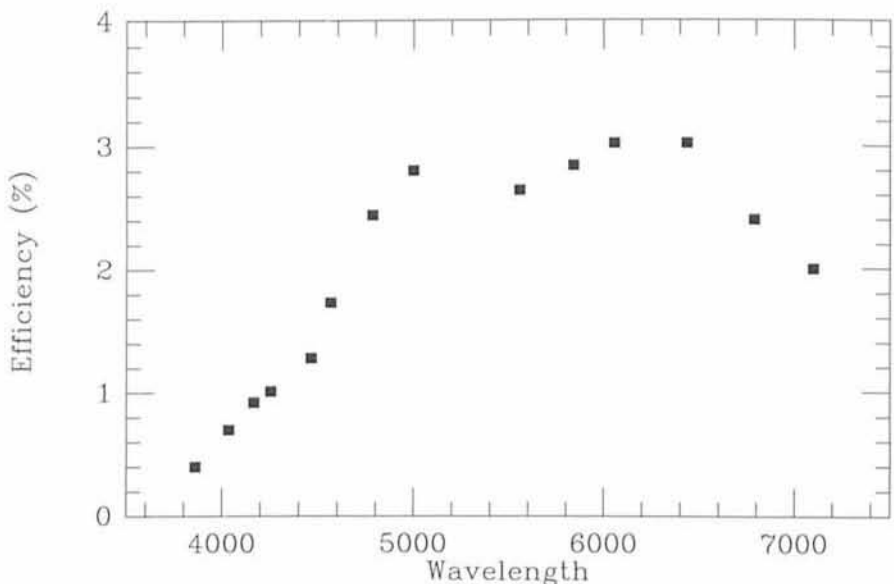


Figure 2: Overall 3.6-m telescope + CASPEC (Short Camera and 31.6 lines/mm echelle) + CCD 16 efficiency curve.

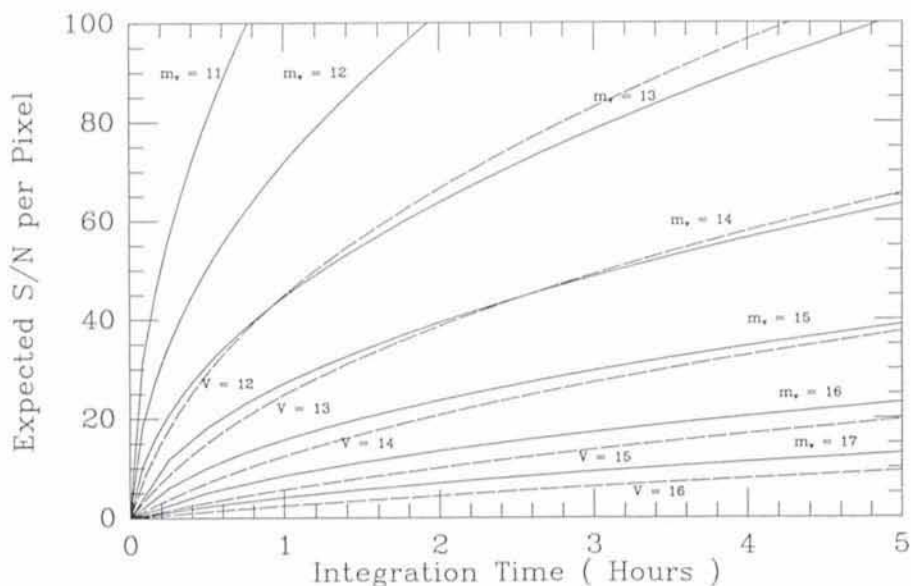


Figure 3: The expected S/N ratios per pixel at 5556 \AA as a function of exposure time for stars of different magnitudes. Continuous lines and m_v refers to the Tektronix chip; dashed lines and V symbols to the RCA. The stellar light was considered to spread over 3 and 4 pixels respectively in the direction perpendicular to the dispersion; pixel size is $27 \times 27 \mu\text{m}$ for the Tektronix and $15 \times 15 \mu\text{m}$ for the RCA.

in the slit (i.e. accurate radial velocities) it is strongly recommended to orient the slit along the parallactic angle.

4. Shifts

It has been known for a long time that CASPEC presented rather pronounced shifts, which were evident whenever the position of the telescope in the sky was changed and during long exposures on faint objects. These shifts were mostly evident in the direction perpendicular to the dispersion and they produced a degradation of the data, spreading the spectrum over several pixels and lowering the effective S/N. These shifts were caused by the servo controlling the crossdisperser; several solutions were attempted and finally a mechanical counterweight has been applied (courtesy of J.L. Lizon).

Tests using calibration-lamp spectra taken at several telescope positions were performed and they showed that the instrument is now very stable (see Fig. 5 for an example). Long exposures on faint sources have confirmed that this problem is now solved.

In order to allow the counterweight to work, the crossdisperser function must be disabled via software; the procedure is described in the CASPEC Manual (Pasquini and D'Odorico, 1989).

5. Maintenance

CASPEC is a rather complex instrument: it has several moving parts, all the functions are remotely controlled, giving the possibility to change central

wavelength and resolution in few minutes; two echelles and two cameras are presently available. Maintenance of such an instrument is therefore a major task. In addition to the regular maintenance, which includes cleaning of the slit jaws, checking and cleaning of all the functions and a new optical alignment, all the mechanical parts close to the beam area were painted black, in order to avoid spurious reflections. This has solved the problem of scattered light affecting the 2-3 bluest orders that appeared when the new CCD (which covers a larger area with respect to the RCA) was used with the 52 lines/mm echelle. New baffles were finally added, in order to make the spectrograph light tight.

Despite the baffling, external light can still penetrate into the spectrograph in presence of a strong source; observers are therefore recommended to switch off the lights in the 3.6-m cage when doing calibrations and dark exposures.

The efficiency of the crossdisperser was checked by observing a standard star at 5050 \AA . It was found to be very close to the manufacturer's specifications, indicating that no degradation has occurred since the first installation of the instrument.

6. Future Improvements

Despite these improvements, some work is still necessary in order to fully exploit the potential of CASPEC and to make it more user friendly; some implementations, concerning a better design of the Rear Slit Viewer, the driving software and the change of some optical parts, are under study.

The first step will consist in the installation of a new RED crossdisperser in the coming months. This crossdisperser will enhance the performance of CASPEC for wavelengths longer than $\sim 5500 \text{ \AA}$, giving a better match between the spectrograph and the chip characteristics. In fact, despite a good quantum efficiency of the Tektronix in the red, the final CASPEC performances are limited in this spectral region by the poor response of the present crossdisperser (Fig. 2.3 in Pasquini and D'Odorico, 1989).

Acknowledgements

We are grateful to J.L. Lizon, G. Rupprecht and S. D'Odorico for their contribution to the improvements of the instrument. CASPEC users deserve special thanks; with their qualified and con-

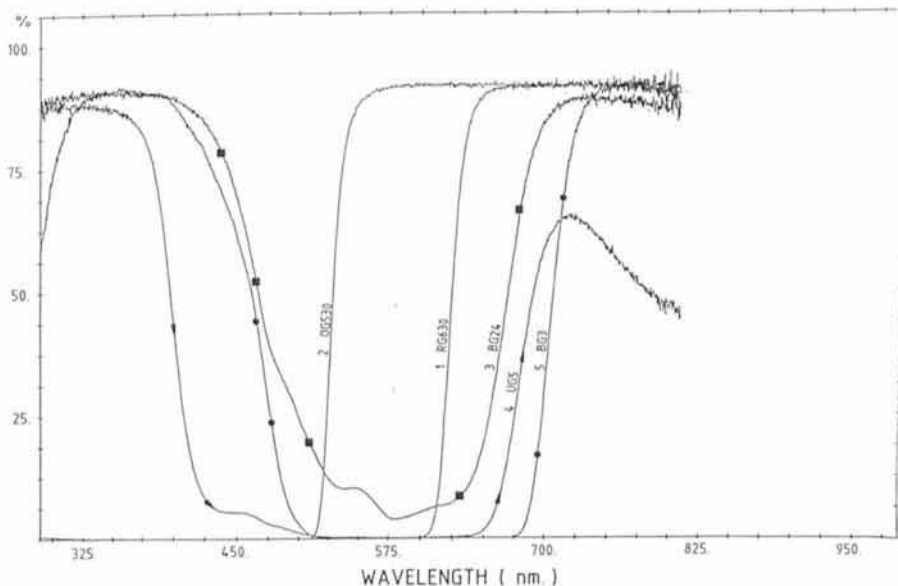


Figure 4: Colour filters response curves as function of wavelength.

CROSS DISPERSION

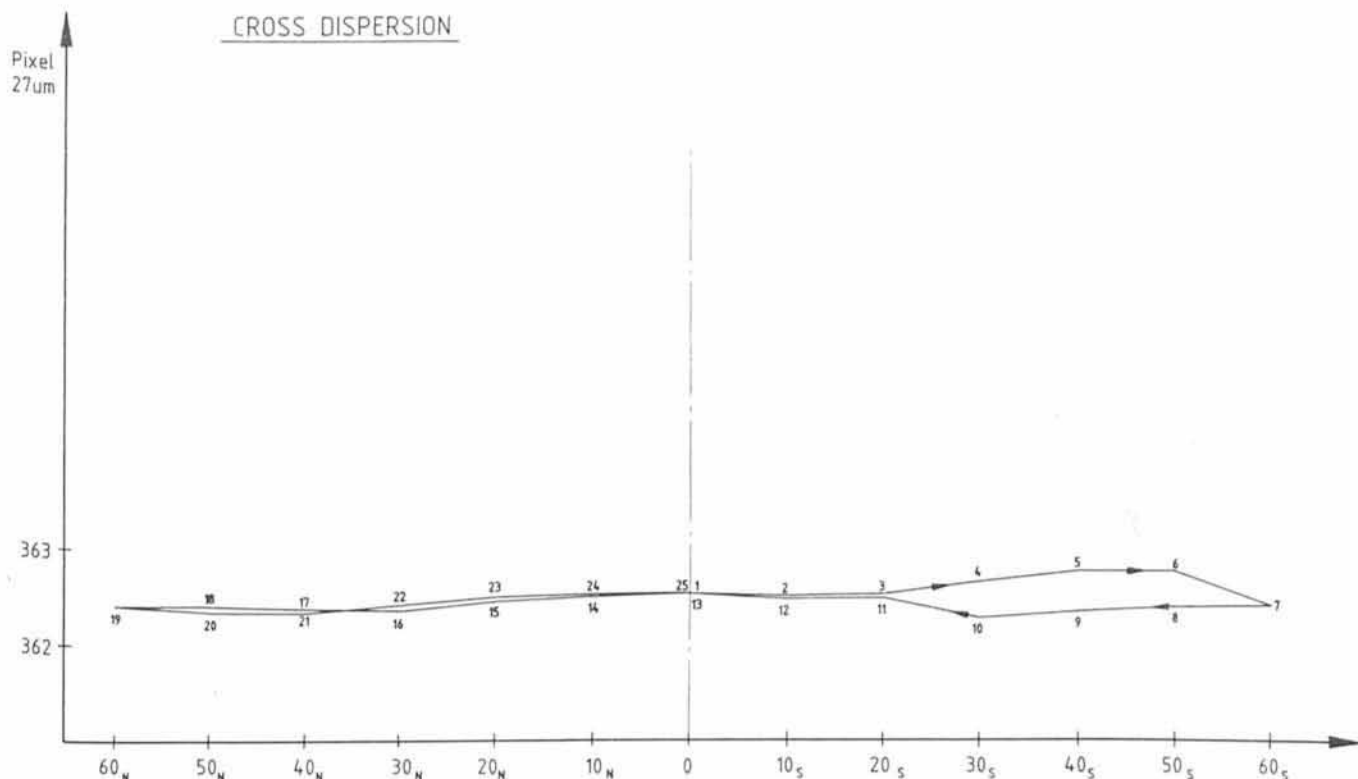


Figure 5: An example of the tests performed to investigate CASPEC shifts: measured pixel positions of a Th-Ar line as a function of the telescope zenith distance. Slit was oriented E-W and the telescope was moved in declination.

structive criticism they greatly contributed to these improvements.

References

Baade, D., Crane, P. 1990: *The Messenger* **61**, 49.

D'Odorico, S. Ghigo, M., Ponz., D. 1987: An Atlas of the Th-Ar Spectrum for the ESO Echelle Spectrograph. ESO Scientific Report **6**.

Pasquini, L., D'Odorico, S. 1989: The CASPEC Operating Manual. ESO Operating Manual **2**.

Sinclair, P. 1991: *CCD detectors available at La Silla*. Third Edition.

Stone, 1977: *Ap. J.* **218**, 767.

Optical Gyros for Astronomical Telescopes

F. MERKLE and M. RAVENBERGEN, ESO

Pointing and tracking of telescopes requires high-precision angular encoders. Up to now classical rotary encoders have been used for this application. Their implementation in modern large telescopes with alt/azimuth mounts becomes rather difficult, because they have to be installed on the rotation axis, which has to be clear and free of any obstruction for the Nasmyth or coudé light path. In the NTT the largest monolithic encoders ever built are used, with a clear inner diameter of 50 cm. Its glass ring, which contains the division scales, has an outer diameter of 70 cm. For the VLT, with Nasmyth beams of approximately 1 m diameter, this type of encoder is not realistic any more and alternatively engraved steel scales mounted on precisely aligned cylinders will be used.

For these reasons, optical gyros have been proposed at ESO as an alternative solution, already in 1986 (1, 2). They have not to be mounted on the rotation axis because they would control the telescope (pointing and tracking) like an

inertial navigation system used in airplanes, satellites, submarines, etc.

In order to assess this new approach and to demonstrate its usefulness for astronomical telescopes, ESO launched a feasibility study in April 1990. The In-

Optical Gyros

Optical gyros (J.R. Wilkinson (1987), *Prog. Quant. Electr.*, Vol. **11**, pp. 1-103) are based on the Sagnac effect (G. Sagnac (1913), *C. R. Acad. Sci.*, Vol. **157**, 708). Two counterpropagating optical waves are travelling inside a ring interferometer and then combined and brought to interference. Is the interferometer not in rotation then the travel time for the two optical paths are the same and the interference pattern at the output is stationary. Is the interferometer rotating around an axis perpendicular to its plane, then one light wave sees its path shortened and the other one sees it elongated. This classical view leads to correct results for the path differences but a detailed physical description has to be based on the general theory of relativity.